Reconnections of Quantized Vortex Rings in Superfluid ^{4}He at Very Low Temperatures

P. M. Walmsley,[1] P. A. Tompsett,[1] D. E. Zmeev,[1,2] and A. I. Golov[1,*]
[1]School of Physics and Astronomy, The University of Manchester, Manchester M13 9PL, United Kingdom
[2]Department of Physics, Lancaster University, Lancaster LA1 4YB, United Kingdom
(Received 2 May 2014; published 17 September 2014)

Collisions in a beam of unidirectional quantized vortex rings of nearly identical radii R in superfluid ^{4}He in the limit of zero temperature (0.05 K) were studied using time-of-flight spectroscopy. Reconnections between two primary rings result in secondary vortex loops of both smaller and larger radii. Discrete steps in the distribution of flight times, due to the limits on the earliest possible arrival times of secondary loops created after either one or two consecutive reconnections, are observed. The density of primary rings was found to be capped at the value 500 $\mathrm{cm}^{-2}R^{-1}$ independent of the injected density. This is due to collisions between rings causing the piling up of many other vortex rings. Both observations are in quantitative agreement with our theory.

DOI: 10.1103/PhysRevLett.113.125302 PACS numbers: 67.25.dk, 47.27.Cn, 47.32.cf

Turbulence appears in various systems—fluids, plasmas, interstellar matter—with common properties such as the existence of long-lived regions of concentrated vorticity, whose reconnections facilitate the evolution of the flow field and redistribution of the kinetic energy between length scales. A paradigm of an isolated vortical structure is a vortex ring [1,2], and their pair interactions are a test bed of the physics of vortex reconnections. Numerical simulations of collisions of two vortex rings predict various outcomes: either a single ring or several rings, depending on the initial conditions [3,4]. There were experimental attempts to visualize these processes in classical fluids [5–7]; however, they are often hard to interpret because of the inevitable decay, core instabilities and poor characterization of vortex rings in viscous fluids.

Quantized vortex rings in superfluids have an advantage because they are slender and stable, and can hence be well characterized quantitatively [8]. Recently, there were many theoretical investigations into reconnections of quantized vortex lines [3,4,9–23]. In particular, for acute angles between two antiparallel reconnecting vortex lines the generation of a cascade of small vortex rings was predicted [20,21,31]. The outcome is reminiscent of that of the Crow instability [24] of antiparallel vortices observed in air. Experimentally, reconnections of vortex lines in superfluid ^{4}He have been visualized [25,26] but only at high temperatures when vortex motion is damped. Reconnections of vortex loops comprising a vortex tangle, i.e., *quantum turbulence* (QT) [27,28], especially those leading to the emission of vortex rings [29], are an important mechanism of redistributing energy towards smaller length scales in QT [30–40].

In superfluid ^{3}He-B [41] and ^{4}He [42], collisions and subsequent reconnections, in a dense beam of vortex rings, generate QT. Longer and more intensive beams of rings result in tangles that show large-scale velocity fluctuations [43,44] and the late-time decay [41,42,45,46], both characteristic of classical turbulence. This implies the existence of the *inverse cascade* of energy from the small length scales (of order ring radii) into which the initial energy is injected—up to the size of the resulting tangle. It was speculated [39] that the inverse cascade might be maintained by the merger of pairs of rings into larger loops. Yet, no direct quantitative observations of ring-ring reconnections have been reported so far.

This Letter reports the first quantitative observations of either one or two consecutive reconnections, and the discovery of the ensuing universal state of depleted density—within a beam of unidirectional quantized vortex rings all of similar radii, with their number density n and radius R under our control. The resulting mechanism of seeding the large-scale velocity fluctuations out of a seemingly random beam of vortex rings is suggested.

In our experiments, to create vortex rings of a required size and to detect their arrival, each was tagged by an excess electron trapped on the vortex core. Applying an electric field along the x axis allowed small seed charged vortex rings (CVRs), injected at $x = 0$, to grow to the desired radius $R(x)$, and also to trace the location of the reconnection process that resulted in small secondary charged vortex rings. The radius of a quantized vortex ring is directly related to its self-induced velocity, $v \sim \kappa/R$, which determines its arrival time at the collector at $x = d$. The numbers of primary and secondary vortex rings as a function of their radii could be extracted from the time dependence of the collector current $I_c(t)$ through time-of-flight spectroscopy. The radius of primary rings at the collector, $R(d)$, was varied within 1–6 μm, with number

density $n(d)$ between 10^4 and 10^7 cm^{-3}, while the mean radius of the seed CVRs was estimated as $\bar{R}_0 \leq 0.5$ μm.

The energy of a CVR, subject to a potential $\phi(x)$, is $\mathcal{E}(x) = \mathcal{E}_0 + e\phi(x)$ in the absence of dissipation at $T < 0.5$ K. The velocity and energy depend on R [2],

$$v = \frac{\kappa}{4\pi R}\left(\Lambda(R) - \frac{1}{2}\right), \qquad \mathcal{E} = \frac{\kappa^2 \rho R}{2}\left(\Lambda(R) - \frac{3}{2}\right), \quad (1)$$

where $\kappa = h/m_4$ is the circulation quantum, ρ is the density of superfluid, $\Lambda = \ln\frac{8R}{a_0}$, and $a_0 = 1.3$ Å [47].

A deeper insight can be gained within the approximation for constant $\Lambda \approx 13$ and uniform field $\phi(x) = \frac{U}{d}x$. The radius of a CVR then grows linearly with x,

$$R(x) \approx R_0 + \frac{2eU}{\rho\kappa^2(\Lambda - 3/2)}\frac{x}{d}, \quad (2)$$

and the time for a CVR to travel from $x = 0$ to $x = d$,

$$\tau_1 \approx \frac{4\pi d}{\kappa(\Lambda - 1/2)}R_0 + \frac{4\pi e d}{\rho\kappa^3(\Lambda - 1)^2}U, \quad (3)$$

increases with energy eU because CVRs slow down as they expand [see Eq. (1)]. In what follows, unless specified, we will be using the approximation $R_0 = 0$.

With increasing density of CVRs, collisions become more frequent. These collisions are caused by small fluctuations in the direction and magnitude of the rings' velocities—mainly due to the variations in initial radii δR_0 and direction of the seed CVRs when injected at $x = 0$. Along with reconnections upon a direct collision, hydrodynamic dipole-dipole interactions between neighboring CVRs (that grow in strength with increasing n and R—and are hence the strongest near the collector at $x \to d$) affect the CVR's velocities. The Coulomb repulsion between neighboring CVRs of $R > 1$ μm is much weaker than their hydrodynamic interaction.

A reconnection of two CVRs results in secondary vortex loops, which are generally noncircular. The two trapped electrons are now carried by either one or by two (if any) of the secondary rings. One special case allows an exact analysis of the consecutive trajectory of one of the electrons—when a secondary CVR has a small initial radius ($R_0 \ll R$). Then its initial deformation and direction of motion can be disregarded, because, under the pull of the electric field, it quickly gains sufficient energy and impulse along the x direction, and so to a good accuracy can be treated as a circular vortex ring [48,49]. If such singly charged loops are created after collisions at some $x = x_1$, their arrival at the collector ($x = d$) at time $\tau_2(x_1) = \tau_1[(\frac{x_1}{d})^2 + (1 - \frac{x_1}{d})^2]$ will be earlier than of any other CVRs with either a larger initial size (slower) or double charge (more energetic, hence, slower). The earliest arrival time,

$$\tau_2^* \equiv \min(\tau_2) = \frac{\tau_1}{2}, \quad (4)$$

will be for collisions at $x_1 = d/2$. Furthermore, if a secondary small ring grows and then reconnects with another vortex loop at some point $x = x_2$ ($x_1 < x_2 < d$), and this creates a new small singly charged ring, the latter will arrive at the collector at time $\tau_3(x_1, x_2) = \tau_1[(\frac{x_1}{d})^2 + (\frac{x_2}{d} - \frac{x_1}{d})^2 + (1 - \frac{x_2}{d})^2]$. The earliest arrival, at time

$$\tau_3^* \equiv \min(\tau_3) = \frac{\tau_1}{3}, \quad (5)$$

of these second-generation secondary CVRs will correspond to two reconnections at $x_1 = d/3$ and $x_2 = 2d/3$.

The experimental cell [50], a cube-shaped volume of side $d = 4.5$ cm, was filled with isotopically pure liquid ^{4}He [51] at pressure 0.1 bar and temperature 0.05 K (see the inset in Fig. 1). Seed CVRs were injected through a gridded opening in the center of one plate. They then traveled along the axis of the container (x axis) towards the center of the opposite plate to the collector electrode, placed behind a Frisch grid of radius $r = 6.5$ mm and geometric transparency $\theta = 0.92$. All currents and potentials are quoted with the opposite sign as if electrons had a *positive* charge e. CVRs were subject to the propelling field set by the potentials of plates $\phi(0) = 0$ and $\phi(d) = U$, thus gaining energy eU while traveling between the injector and collector grids [52]. The dependence $\phi(x)$ was close to the linear $\phi = U\frac{x}{d}$ (see the inset in Fig. 2).

The seed CVRs resulted from reconnections within the dense vortex tangle, generated by the current of electrons emitted from a tungsten tip [55] behind the injector grid through the voltage $U_{\rm tip}$. These seed CVRs are injected in a broad range of angles; however, the impulse gained from the strong driving field quickly forces them to travel in nearly the same x direction with a relatively narrow distribution of radii. The intensity and duration of the injected pulse were controlled by adjusting $U_{\rm tip}$ and its

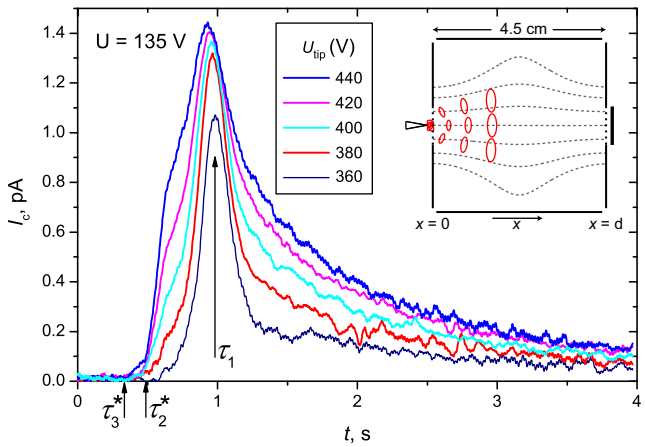

FIG. 1 (color online). Records of collector current, all for the same drive voltage $U = 135$ V, but for different tip voltages $U_{\rm tip}$. The theoretical arrival time for primary CVRs, τ_1 [Eq. (3)], and of the earliest arriving secondary CVRs of the first generation, τ_2^* [Eq. (4)], and of the second generation, τ_3^* [Eq. (5)], are shown by arrows. Inset: Experimental cell with an electric field pattern.

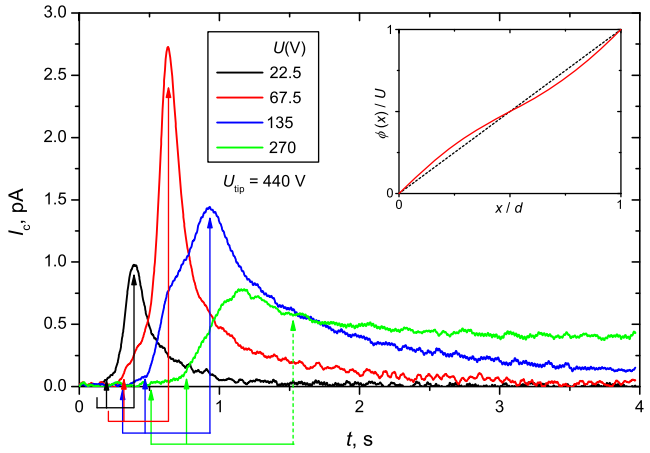

FIG. 2 (color online). Records of the collector current, all for the same $U_{tip} = 440$ V, but different values of U. The right, middle, and left arrows of the corresponding colors point at the arrival time of primary CVRs, τ_1, and the theoretical earliest arrival times for secondary CVRs of the first [Eq. (4)] and second [Eq. (5)] generations, respectively. The values of τ_1 are defined as the positions of sharp peaks, except for $U = 270$ V—where the peak due to primary CVRs is swamped by the broad pedestal due to secondary CVRs; hence, the theoretical value of τ_1 [see Fig. (3)] is used. For $U = 22.5$ and 67.5 V, the signal is too faint for the step at τ_3^* to be observable. Inset: The electrostatic potential $\phi(x)$ along the cell's axis.

duration Δt (all data presented here are for $\Delta t = 0.2$ s). For the same U_{tip} and Δt, the total charge injected through the grid was increasing with an increasing drive voltage U nearly linearly for all studied voltages. To quantify the time of flight τ_1 of CVRs, we take the time interval between the middle of the tip voltage pulse and the position of the maximum of $I_c(t)$ (and subtract the electronics response time of 0.03 s).

Typical records of the collector current, $I_c(t)$, following the injection of a pulse of CVRs are shown in Fig. 1. These are all for the same drive voltage $U = 135$ V but several different injection currents. There is a well-defined peak at time $\tau_1 \approx 1.0$ s corresponding to the arrival of primary CVRs. With increasing density of CVRs, this peak initially grows in magnitude while maintaining its position, τ_1, and width, $\sim\Delta t$. At higher numbers of injected CVRs, however, a broad pedestal begins to grow, coexisting with the original peak (whose magnitude is now saturated). This broad pedestal is due to the secondary CVRs that result from collisions between primary CVRs. The current at $t > \tau_1$ reflects the arrivals of larger secondary vortex loops, while that at the earlier arrival times $t < \tau_1$ are from smaller secondary CVRs. A sharp step builds up at $\tau_2^* = \tau_1/2$, coinciding with the earliest possible arrival of the first generation of secondary CVRs [Eq. (4)]. At the highest intensity of injection, another sharp step begins to form at $\tau_3^* = \tau_1/3$, corresponding to the earliest possible arrival of the second generation of secondary CVRs [Eq. (5)].

In Fig. 2, we show $I_c(t)$, similar to those in Fig. 1, but now for the same tip voltage $U_{tip} = 440$ V and four different drive voltages U. With increasing U, the position of the peak τ_1 increases as expected for isolated CVRs, Eq. (3). The peak's magnitude $I_m(U)$ initially grows with U but then, above $U = 68$ V, decreases—even though the total collected charge $Q_c = \int_0^\infty I_c(t)dt$ keeps increasing. Simultaneously, the broad pedestal due to secondary CVRs progressively overgrows the primary peak until completely swamping it at $U = 270$ V. The sharp steps due to the earliest possible arrivals of secondary CVRs of the first generation at $\tau_1/2$ [Eq. (4)] and second generation at $\tau_1/3$ [Eq. (5)] are labeled by arrows. We thus obtained quantitative evidence of either single or two consecutive reconnections of CVRs during their motion from the injector to collector. Furthermore, the substantial contribution to the collector current right after the cutoffs indicates that very small CVRs are created with high probability. This might contradict the expectations that reconnections result in vortex loops of a size *comparable* to the radius of curvature of the initial vortex lines [33,36], but would support the picture of a cascade of small vortex rings created by large-amplitude Kelvin waves generated after a reconnection of nearly antiparallel vortex lines when dissipation is small [20,21,31].

In Fig. 3, the experimental arrival times $\tau_1(U)$ for several intensities of the injection are plotted. For small drive voltages U [i.e., when the radii of CVRs $R(d)$ and density of CVRs $n(d)$ are small] the experimental points agree with the theory for isolated CVRs [from Eqs. (1)–(2)]. To characterize the range of the distribution of times of flight,

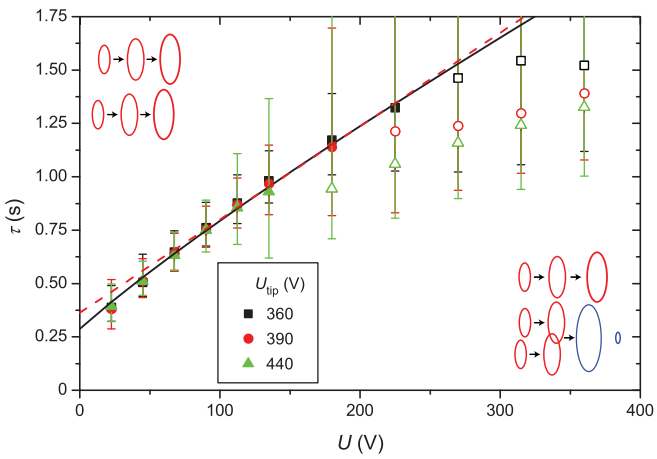

FIG. 3 (color online). The elapsed times between the middle of the emitter pulse and maximum of $I_c(t)$ vs U. Closed symbols correspond to resolvable sharp peaks due to primary CVRs; open symbols are for the broadened peaks due to secondary CVRs where sharp peaks due to primary CVRs are no longer visible. Vertical bars indicate the peak width at half-maximum. The solid line shows the theoretical arrival times τ_1 [Eqs. (1)–(2)] for $R_0 = 0.5$ μm. The dashed line shows the approximate solution for $\Lambda = 13$ and effective $R_0 = 0.8$ μm [Eq. (3)]. Cartoons illustrate the expansion and progression of (left) isolated primary (red) CVRs at low density, and (right) a reconnection resulting in secondary (blue) CVRs.

the vertical bars show the width of $I_c(t)$ at the $0.5I_m$ level. One can see that at small U the width is constant, being equal to the injection duration $\Delta t = 0.2$ s. Above a certain value of $U \sim 100$ V (that decreases with the increasing injection intensity, $U_{\rm tip}$), the collector pulse broadens and the position of the maximum of $I_c(t)$ no longer agrees with the theoretical prediction for isolated CVRs (this coincides with the complete disappearance of the sharper peak due to primary CVRs, as on the trace for $U = 270$ V in Fig. 2); secondary CVRs dominate $I_c(t)$ in these conditions of high n and R.

The density of primary rings reaching the collector, $n_1 \equiv n(d)$, can be found from the value of the collector current at its maximum [but only for the records $I_c(t)$ that have a sharp peak at $t = \tau_1$, dominant over the pedestal due to the secondary CVRs],

$$I_m \approx \theta\pi r^2 e n_1 v_1 \approx \frac{1}{8}\theta r^2 \rho\kappa^3(\Lambda-1)^2\frac{n_1}{U}, \qquad (6)$$

where the relation $v_1 \equiv v(d) \approx (\rho\kappa^3(\Lambda-1)^2)/(8\pi eU)$ [from Eqs. (1)–(2)] has been used. In Fig. 4, we plot n_1 [calculated from the experimental values of $I_m(U)$ using Eq. (6)] vs $R_1 \equiv R(d)$, the radii of primary CVRs near the collector [calculated from Eq. (2) with $R_0 = 0$). Again, there are two regimes: at low R_1, n_1 increases with an increase of either $U_{\rm tip}$ or U, but at large R_1, n_1 becomes a *decreasing* function of U, independent of $U_{\rm tip}$. Yet, the total injected charge (as measured by the integral of the collector current) increases monotonically at all U. In other words, only at small R_1 and n_1 can the CVR's density be controlled by varying the injection current. At high R_1, only a small fraction of charge arrives with primary CVRs of now *universal* density $n_1 \approx 500$ cm$^{-2}R_1^{-1}$; the rest (secondary CVRs) contribute to the broad pedestal in $I_c(t)$ (Figs. 1, 2).

The density of primary rings in the beam $n(x,t)$, along the trajectory $x(t)$, evolves according to Eq. (11) in [56]:

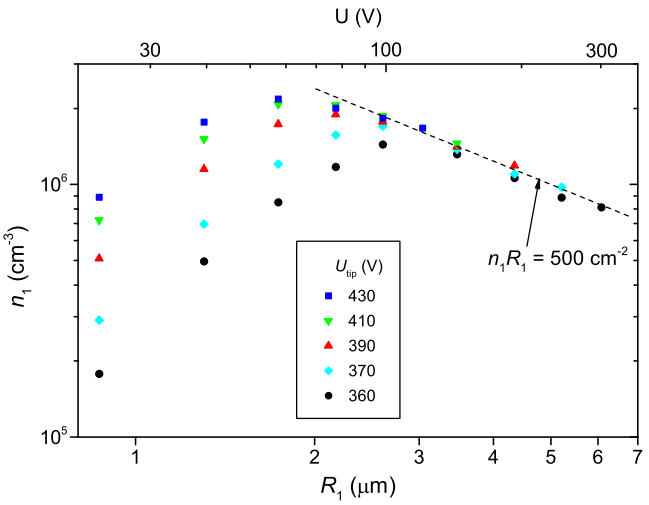

FIG. 4 (color online). Density of primary CVRs n vs their radius R at $x = d$ measured for several different drive voltages U (top axis) and injector tip voltages, $U_{\rm tip}$ (see legend).

$$\frac{dn}{dt} = -n\frac{dv}{dx} - f, \qquad (7)$$

where $-f$ is the rate of losses per unit volume and time, due to ring-ring collisions. For small injected density and radii, the collisions can be neglected, $f = 0$, and the solution for the density near the collector is

$$n_1 = \frac{8\pi I_m U}{\theta\pi r^2\rho\kappa^3(\Lambda-1)^2}; \qquad (8)$$

i.e., it can be varied by changing either the injected density of CVRs (characterized by I_m) or drive voltage U—as observed in the experiment. When collisions become rife at higher densities and radii, accounting for the removal of primary CVRs due to their binary collisions results in

$$n_1R_1 = \frac{3}{\sigma_1'\delta R d} = 4\times10^3 \text{ cm}^{-2}, \qquad (9)$$

where we used $\delta R = 0.5$ μm and the geometric cross section for collisions $\sigma_1 = \sigma_1' R^2$ with $\sigma_1' = 4\pi$. Furthermore, the subsequent removal of primary CVRs that bump into the slower loops [57] left after the described collisions of primary CVRs will result in the solution,

$$n_1R_1 = \left(\frac{40\pi}{(\Lambda-1/2)\kappa\sigma_1'\sigma_2'\delta R\Delta t d}\right)^{1/2} = 1\times10^3\,\text{cm}^{-2}, \qquad (10)$$

where the geometric cross section for these pileups is estimated as $\sigma_2 = \sigma_2' R^2$ with $\sigma_2' = 4\sqrt{2}\pi$. Both Eqs. (9) and (10) reproduce the experimental universal dependence $n_1R_1 = 500$ cm^{-2} qualitatively, while Eq. (10) is actually quite close *quantitatively* (our one-dimensional model underestimates f by disregarding the transverse component of the relative motion of primary CVRs and hence overestimates the value of n_1R_1 by a factor of 2 or so [56]).

The fact of occasional piling up of many primary CVRs, in turn, helps to explain the appearance of large-scale velocity fluctuations in the ensuing vortex tangle. In the initial random beam of primary CVRs, the fluctuations of the coarse-grained velocity on the length scales greater than $\sim n^{-1/3}$ ("quasiclassical" flow) are small; the energy spectrum is concentrated around the small length scale of order R. The small secondary vortex rings, observed in this work, and Kelvin waves excited by reconnections are evidence of the direct cascade of energy towards smaller length scales [31–33,35,36,40]. However, following any of the pileups of many vortex rings, strong fluctuations of the coarse-grained velocity field on the quasiclassical length scales $\gg n^{-1/3}$ are being created. This is the inverse cascade of energy in this strongly anisotropic system [37,39].

To summarize, we obtained quantitative evidence for collisions and reconnections of pairs of unidirectional vortex rings of similar radii that result in the creation of vortex loops of unequal size, including many small ones. We observed discrete steps at the time dependence of the collector current, which correspond to the earliest arrivals

of the first and second generations of secondary CVRs. As each collision can cause a removal of many primary vortex rings, increasing the density of injected CVRs results in a new state in which the density of primary vortex rings is maintained at the critically depleted level independent of their initial density. The larger loops produced in the collisions become the seeds of quasiclassical QT with large-scale flow structures, which appear out of a seemingly random beam of small quantized vortex rings.

This work was supported by the Engineering and Physical Sciences Research Council (Grants No. GR/R94855, No. EP/H04762X/1, and No. EP/I003738/1).

*Corresponding author.
andrei.golov@manchester.ac.uk

[1] K. Shariff and A. Leonard, Annu. Rev. Fluid Mech. **24**, 235 (1992).
[2] C. F. Barenghi and R. J. Donnelly, Fluid Dyn. Res. **41**, 051401 (2009).
[3] J. Koplik and H. Levine, Phys. Rev. Lett. **76**, 4745 (1996).
[4] D. Kivotides and A. Leonard, Phys. Rev. Lett. **90**, 234503 (2003).
[5] T. Kambe and T. Takao, J. Phys. Soc. Jpn. **31**, 591 (1971).
[6] T. Fohl and J. S. Turner, Phys. Fluids **18**, 433 (1975).
[7] Y. Oshima and S. Asaka, J. Phys. Soc. Jpn. **42**, 708 (1977).
[8] G. W. Rayfield and F. Reif, Phys. Rev. **136**, A1194 (1964).
[9] A. Pumir and R. M. Kerr, Phys. Rev. Lett. **58**, 1636 (1987).
[10] J. Koplik and H. Levine, Phys. Rev. Lett. **71**, 1375 (1993).
[11] C. Nore, M. Abid, and M. E. Brachet, Phys. Rev. Lett. **78**, 3896 (1997).
[12] D. Kivotides, J. C. Vassilicos, D. C. Samuels, and C. F. Barenghi, Phys. Rev. Lett. **86**, 3080 (2001).
[13] M. Leadbeater, T. Winiecki, D. C. Samuels, C. F. Barenghi, and C. S. Adams, Phys. Rev. Lett. **86**, 1410 (2001).
[14] M. Leadbeater, D. C. Samuels, C. F. Barenghi, and C. S. Adams, Phys. Rev. A **67**, 015601 (2003).
[15] P. Chatelain, D. Kivotides, and A. Leonard, Phys. Rev. Lett. **90**, 054501 (2003).
[16] A. Mitani and M. Tsubota, Phys. Rev. B **74**, 024526 (2006).
[17] S. K. Nemirovskii, Phys. Rev. Lett. **96**, 015301 (2006).
[18] C. F. Barenghi, R. Hänninen, and M. Tsubota, Phys. Rev. E **74**, 046303 (2006).
[19] S. Z. Alamri, A. J. Youd, and C. F. Barenghi, Phys. Rev. Lett. **101**, 215302 (2008).
[20] R. M. Kerr, Phys. Rev. Lett. **106**, 224501 (2011).
[21] M. Kursa, K. Bajer, and T. Lipniacki, Phys. Rev. B **83**, 014515 (2011).
[22] R. Hänninen, Phys. Rev. B **88**, 054511 (2013).
[23] R. M. Caplan, J. D. Talley, R. Carretero-Gonzalez, and P. G. Kevrekidis, arXiv:1404.4922v1.
[24] S. C. Crow, AIAA J. **8**, 2172 (1970).
[25] G. P. Beweley, M. S. Paoletti, K. R. Sreenivasan, and D. P. Lathrop, Proc. Natl. Acad. Sci. U.S.A. **105**, 13707 (2008).
[26] E. Fonda, D. P. Meichle, N. T. Ouellette, S. Hormoz, and D. P. Lathrop, Proc. Natl. Acad. Sci. U.S.A. **111**, 4707 (2014).
[27] K. W. Schwarz, Phys. Rev. B **38**, 2398 (1988).
[28] W. F. Vinen and J. J. Niemela, J. Low Temp. Phys. **128**, 167 (2002).
[29] Y. Nago, A. Nishijima, H. Kubo, T. Ogawa, K. Obara, H. Yano, O. Ishikawa, and T. Hata, Phys. Rev. B **87**, 024511 (2013).
[30] H. Salman, Phys. Rev. Lett. **111**, 165301 (2013).
[31] B. V. Svistunov, Phys. Rev. B **52**, 3647 (1995).
[32] M. Tsubota, T. Araki, and S. K. Nemirovskii, Phys. Rev. B **62**, 11751 (2000).
[33] C. F. Barenghi and D. C. Samuels, Phys. Rev. Lett. **89**, 155302 (2002).
[34] S. K. Nemirovskii, Phys. Rev. B **77**, 214509 (2008).
[35] S. K. Nemirovskii, Phys. Rev. B **81**, 064512 (2010).
[36] E. Kozik and B. Svistunov, Phys. Rev. B **77**, 060502(R) (2008).
[37] S. Yamamoto, M. Tsubota, and W. F. Vinen, J. Phys. Conf. Ser. **400**, 012075 (2012).
[38] L. Kondaurova and S. K. Nemirovskii, Phys. Rev. B **86**, 134506 (2012).
[39] A. W. Baggaley, C. F. Barenghi, and Y. A. Sergeev, Phys. Rev. B **85**, 060501 (2012); Phys. Rev. E **89**, 013002 (2014).
[40] S. Nazarenko, JETP Lett. **84**, 585 (2007).
[41] D. I. Bradley, D. O. Clubb, S. N. Fisher, A. M. Guénault, R. P. Haley, C. J. Matthews, G. R. Pickett, V. Tsepelin, and K. Zaki, Phys. Rev. Lett. **95**, 035302 (2005).
[42] P. M. Walmsley and A. I. Golov, Phys. Rev. Lett. **100**, 245301 (2008).
[43] D. I. Bradley, S. N. Fisher, A. M. Guénault, R. P. Haley, S. O'Sullivan, G. R. Pickett, and V. Tsepelin, Phys. Rev. Lett. **101**, 065302 (2008).
[44] P.-E. Roche and C. F. Barenghi, Europhys. Lett. **81**, 36002 (2008).
[45] A. I. Golov and P. M. Walmsley, J. Low Temp. Phys. **156**, 51 (2009).
[46] P. Walmsley, D. Zmeev, F. Pakpour, and A. Golov, Proc. Natl. Acad. Sci. U.S.A. **111**, 4691 (2014).
[47] W. I. Glaberson and R. J. Donnelly, *Structure, Distribution, and Dynamics of Vortices in Helium II*, edited by D. F. Brewer, Progress in Low Temperature Physics, Vol. 9 (North-Holland, Amsterdam, 1986).
[48] D. C. Samuels and R. J. Donnelly, Phys. Rev. Lett. **67**, 2505 (1991).
[49] M. Tsubota and H. Adachi, J. Low Temp. Phys. **158**, 364 (2010).
[50] P. M. Walmsley, A. A. Levchenko, S. E. May, and A. I. Golov, J. Low Temp. Phys. **146**, 511 (2007).
[51] Helium gas with ^{3}He concentration less than 2×10^{-11} was produced at Lancaster University by the technique published in P. C. Hendry and P. V. E. McClintock, Cryogenics **27**, 131 (1987).
[52] This is similar to the dynamics of classical buoyant vortex rings [53,54].
[53] J. S. Turner, Proc. R. Soc. A **239**, 61 (1957).
[54] D. Bond and H. Johari, Exp. Fluids **48**, 737 (2010).
[55] A. Golov and H. Ishimoto, J. Low Temp. Phys. **113**, 957 (1998).
[56] See the Supplemental Material at http://link.aps.org/supplemental/10.1103/PhysRevLett.113.125302 for our analytical calculations of the effect of collisions of primary CVRs on their density at collector.
[57] These secondary collisions were envisaged in [41,58].
[58] S. Fujiyama, A. Mitani, M. Tsubota, D. I. Bradley, S. N. Fisher, A. M. Guénault, R. P. Haley, G. R. Pickett, and V. Tsepelin, Phys. Rev. B **81**, 180512(R) (2010).